THE JOURNAL OF INVESTIGATIVE DERMATOLOGY, 68:73-78, 1977

Vol. 68, No. 2
Printed in U.S.A.

STEREOLOGIC BASELINE DATA OF NORMAL HUMAN EPIDERMIS

A. J. P. KLEIN-SZANTO, M.D.

Department of Oral Structural Biology, University of Zurich Dental Institute, Zurich, Switzerland, and Department of Radiobiology, National Atomic Energy Commission, Buenos Aires, Argentina

Stereologic techniques for electron microscopic morphometry have been applied to normal human interfollicular epidermis of the submammary and iliac crest regions. The aim was to obtain objective baseline data for the study of epidermal morphometric pathology. The results, expressed mainly in surface, volume, and numerical densities of epidermal components and keratinocyte organelles, revealed ascending or descending gradients throughout the epithelial strata. The cytoplasmic ground substance remained almost constant in the four studied layers. No important regional differences were found between the epidermal morphometric parameters at either site. The epidermis showed striking volumetric composition similarities with other keratinizing epithelia.

Variations in the relative composition of keratinocyte components in experimental and spontaneous pathologic conditions frequently have been reported on the basis of subjective evaluation of electron micrographs. By this procedure quantitative changes in the cytoplasmic content of tonofilaments, mitochondria, keratinosomes, and other organelles have been postulated in as different conditions as lichen planus, psoriasis vulgaris, horny layer stripped epidermis, irradiated epidermis, and many other lesions [1-9].

The application of modern stereologic techniques of ultrastructural morphometry [10] to several normal tissues yielded an objective quantitative description of membrane surfaces and submicroscopic volumes. These studies have been performed with many different mammalian tissues [11-17] serving as baseline data for comparative studies where the morphometric analysis of the same tissues under experimental conditions or in disease states was carried out [18-24].

Although light microscopic histometry and electron microscopic quantitation of some specific cutaneous features have been reported [25-34], a complete stereologic analysis of normal human epidermis has not, to my knowledge, been carried out. This study represents an attempt to describe in a quantitative and objective way the ultramorphologic features of human epidermis, in order to furnish baseline data for the study of epidermal morphometric pathology. The study was developed and carried out taking into account the previous experience in the stereologic assessment of normal squamous epithelia of the oral mucosa [35-41].

Manuscript received April 15, 1976; accepted for publication September 8, 1976.

This study was supported in part by grant No. 106 of the Hartmann-Muller Foundation for Scientific Research and by a grant from the Stiftung fur Wissenschaftliche Forschung an der Universitat Zurich assigned to Dr. Schroeder.

Reprint requrests to: Dr. A. J. P. Klein-Szanto, Department of Radiobiology, C.N.E.A., Avda. del Libertador 8250, 1429 Buenos Aires, Argentina.

MATERIAL AND METHODS

Biopsies

Nine skin surgical biopsies, 4 from the submammary region and 5 from the iliac crest region, were obtained from female patients (age range 19 to 23 years) undergoing plastic surgery. The biopsies were immediately placed in chilled half-strength Karnovsky fixative [42] and subdivided into 5 to 7 approximately 1-mm-thick blocks, cut perpendicularly to the surface.

After 2 hr the blocks were washed in 0.18 M cacodylate buffer and postfixed in 1.33% osmic acid buffered (pH 7.4) in 0.067 M *s*-collidine at 4°C, thereafter dehydrated in ethanol, and embedded in Epon [43]. The tissue blocks were orientated flat at the bottom of reversed BEEM capsules. From a total of 47 blocks, 1-μm-thick sections were prepared and stained with PAS-toluidine blue-azure II [44]. From these blocks, 3 out of each biopsy were selected on the criteria of the best tissue orientation and preservation of the interfollicular epidermis, and served for both epithelial thickness measurements and stereologic analysis. Measurements of epithelial thickness were performed in regions of epithelial ridges, over connective tissue papillae, and at random [37]. (The stratum corneum was measured separately.)

Ultrathin sections were cut and processed according to a previously published sequence [41].

Sampling and Stereologic Procedures

Electron micrographs were recorded following an already described sampling design based on a model of stratification [40-41].* In brief, it was performed on two levels of magnification and four epithelial strata. In the submammary epidermis the four strata represented an almost consecutive field-to-field sample at the lower level of magnification. In the iliac crest epidermis, which was slightly thicker, small areas between the strata were equidistantly excluded from the stereologic analysis.

Level I magnification: Six electron micrographs at a primary magnification of 3070× were recorded in each stratum and for each block. Thus three times 24 photos

* Hammer B, Schroeder HE: On-line computer program for stereologic analysis of oral epithelia, based on a model of stratification (in preparation).

were collected per block, yielding a total of 288 negatives for the submammary epidermis group (4 biopsies × 3 blocks × 4 strata × 6 micrographs) and 360 electron micrographs for the iliac crest epidermis group (5 biopsies × 3 blocks × 4 strata × 6 micrographs).

Level II magnification: Twelve micrographs were recorded using a primary magnification of 6070× within the strata sampled at level I. In total, 48 electron micrographs were sampled from each block, yielding a total of 576 negatives for the submammary epidermis (4 biopsies × 3 blocks × 4 strata × 12 micrographs) and 720 negatives for the iliac crest epidermis (5 biopsies × 3 blocks × 4 strata × 12 micrographs).

Two additional series of electron micrographs were recorded for the measurement of cytoplasmic filament diameter and basal lamina thickness [41].

The quantitative analysis was carried-out using a coherent double-lattice test system with 99 heavy points and 891 light points respectively [10]. The application of this test system on squamous epithelia and the subsequent data recording as well as computation and statistical analysis have already been reported [40,41].

RESULTS

General Description of the Epidermis

The interfollicular epidermis of the submammary region was found to be of rather similar thickness and structure as the one of the iliac crest region. Although the latter was slightly thicker and presented more epithelial ridges interdigited with a somewhat denser dermal papillary body, the overall architecture, differentiation pattern, and horny layer formation were similar in both regions (Fig. 1, Tab. I).

The basal complex beneath the epithelium was composed of a very distinct lamina lucida and a lamina densa of approximately equal thickness in both skin regions under study (lamina densa 540 to 580 Å, lamina lucida 370 to 390 Å).

Composition of Epidermis

Table II summarizes the stereologic data of epidermis at both locations expressing the morphometric parameters of epithelial tissue components per unit volume of total epidermal tissue. The epidermis of both sites showed similar characteristics, i.e., both revealed the same pattern of epidermal component variations throughout the strata, from the basal to the granular layers. (Fig. 1). These variations consisted mainly of: a marked decrease of the relative volume of nuclei (from approximately 26% in the basal layer to 5% in the granular layer), a decrease of the relative volume of the metabolically active organelles (from 8% to 4% in the basal and granular layers, respectively), an increase in the volume density of filament bundles (from approximately 15% in the basal layer to 27% in the granular layer), decreasing volume densities of intercellular space and nonkeratinocytes, and only a slight increase in the relative volume of the cytoplasmic ground substance.

The number of desmosomes increased approximately 4 times from the basal to the granular layer (12 desmosomes/100 μm^2 field in the stratum basale to 47 desmosomes/100 μm^2 field in the stratum granulosum). The nucleus to cytoplasm volume, and surface ratios, decreased in a similar pattern from the basal layer to the surface (from approximately 0.4 in the basal layer to 0.06 in the granular layer).

TABLE I. *Epidermal thickness (in μm)*

	Iliac crest region	Submammary region
In epithelial ridges	119 ± 8	104 ± 15
Over connective tissue papillae	42 ± 3	38 ± 7
Random	81 ± 5	56 ± 10
Stratum corneum	7 ± 1	7 ± 1

Organelle Density Gradients

In order to eliminate the variations in strata composition caused by the heterogeneous distribution of the intercellular space, nonkeratinocytes, and nuclear volume fractions, and to compare the data of epidermis at the two different sites, the results were expressed in relation to one unit volume of epithelial cytoplasm. Figures 2 and 3 show gradients of the most important cytoplasmic constituents.

The mitochondrial, ribosomal, and endoplasmic reticulum volume fractions showed a marked decrease from the basal to the granular layer. Slightly decreasing gradients could be observed in the volume densities of the Golgi apparatus and cytoplasmic vesicles. The volume fraction occupied by bundled filaments increased from the basal to the upper spinous layer, exhibiting a relative decrease in the granular layer. Non-bundled cytoplasmic filaments were present in the basal layer only, accounting for 0.7% and 1.5% of the cytoplasmic volume in the submammary and iliac crest epidermis, respectively. The diameters of single cytoplasmic filaments were similar at both sites and in all strata (range, 72 to 86 Å).

The volume density of the membrane-coating granules increased gradually up to the lower spinous layer and markedly throughout the two remaining superficial strata. Keratohyalin was present in the granular layer only, representing 5% of the cytoplasmic volume. The volume fraction of the cytoplasmic ground substance remained relatively constant throughout the four layers.

Differences in volume densities of cytoplasmic components between the two epidermal localizations were insignificant.

DISCUSSION

Previous descriptions of the ultrastructural aspects of epidermis have been essentially qualitative. While subjective observations are necessary in order to provide an initial estimation of the cellular ultrastructure and of epidermal differentiation, an objective quantitative analysis of systematically sampled tissue is an unavoidable step to obtain meaningful and unbiased data on the epidermal cytoarchitecture. In this way subjective

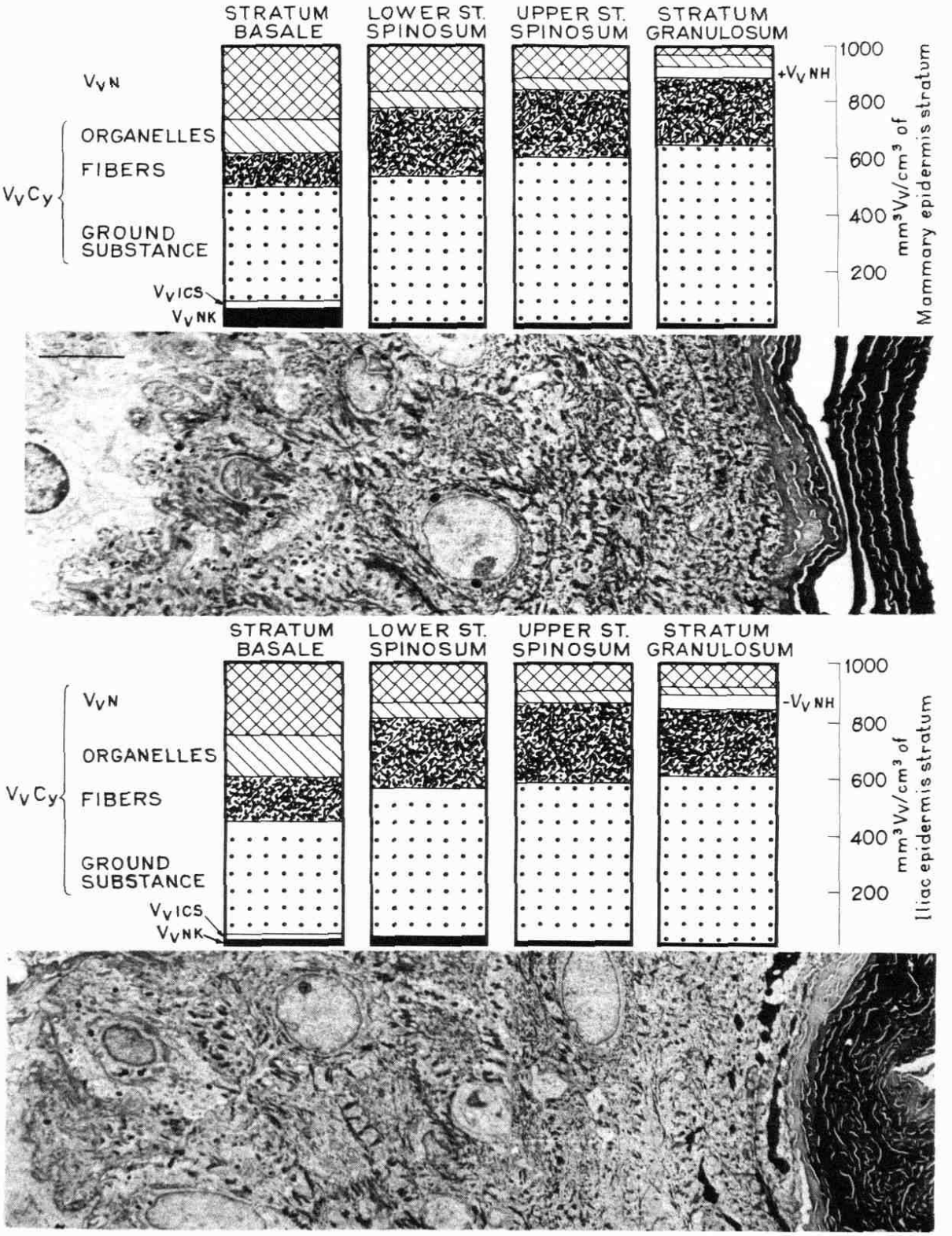

FIG. 1. Composition of submammary (*upper part*) and iliac crest region (*lower part*) epidermis. For each of the four strata the epidermal constituents are expressed in mm^3 per 1 cm^3 of epidermal stratum (for abreviations see Table II) (× 2700). Bar = 5 μm.

factors which can distort the real biostructural composition of the epithelium are eliminated, yielding reliable data adequate for comparative purposes. This type of morphometric evaluation recently has been applied to the analysis of numerous pathologic and experimental conditions in liver, lung, kidney [18–24], and many other tissues including oral mucosa [40].

The present study provides stereologic baseline data of the normal human epidermis for compari-

TABLE II. *Sterologic parameters of normal epidermis at two different sites*

Parameter[a]	Stratum basale		Stratum spinosum (L)		Stratum spinosum (U)		Stratum granulosum	
	Submammary region	Iliac crest region	Submammary region	Iliac crest region	Submammary region	Iliac crest region	Submammary region	Iliac crest region
S_v PM	0.74 ±0.07	0.91 ±0.19	1.08 ±0.21	1.13 ±0.18	1.11 ±0.10	1.21 ±0.24	0.99 ±0.10	1.01 ±0.15
V_v ICS	2.47 ±3.21	0.61 ±0.81	1.87 ±2.20	0.73 ±0.91	0.90 ±1.09	1.48 ±1.90	0.03 ±0.06	–
V_v NK	101.00 ±52.00	33.00 ±39.00	4.63 ±3.47	24.20 ±24.80	2.74 ±2.73	3.30 ±2.20	0.42 ±0.84	0.56 ±1.12
V_v N	259.00 ±32.00	275.00 ±62.00	154.00 ±86.00	125.00 ±43.00	118.00 ±53.00	105.00 ±53.00	40.00 ±15.00	71.00 ±26.00
S_v NM	0.30 ±0.06	0.31 ±0.09	0.18 ±0.08	0.15 ±0.05	0.12 ±0.06	0.15 ±0.04	0.05 ±0.01	0.08 ±0.04
V_v CY	636.00 ±36.00	6.90 ±49.00	838.00 ±89.00	850.00 ±46.00	877.00 ±55.00	890.00 ±50.00	959.00 ±15.00	926.00 ±25.00
V_v MI	19.07 ±4.18	19.10 ±2.72	19.09 ±4.75	17.62 ±5.82	12.62 ±4.84	12.00 ±5.77	10.76 ±4.67	10.04 ±2.08
V_v RIB	24.86 ±4.32	24.00 ±3.42	28.29 ±3.73	23.30 ±2.83	20.01 ±2.77	22.00 ±6.44	20.66 ±3.81	21.00 ±3.69
V_v ER	3.53 ±1.29	6.68 ±3.74	1.43 ±1.53	1.42 ±1.97	0.53 ±0.45	1.31 ±1.28	0.60 ±0.43	0.59 ±0.40
S_v ER	0.27 ±0.07	0.31 ±0.17	0.08 ±0.09	0.07 ±0.09	0.03 ±0.02	0.06 ±0.05	0.03 ±0.02	0.02 ±0.02
V_v GO	0.65 ±0.32	0.71 ±0.44	0.50 ±0.20	0.51 ±0.30	0.43 ±0.30	0.90 ±0.57	0.39 ±0.30	0.75 ±0.31
S_v GO	0.06 ±0.03	0.05 ±0.05	0.03 ±0.01	0.03 ±0.02	0.02 ±0.02	0.04 ±0.02	0.02 ±0.01	0.03 ±0.01
V_v VES	1.17 ±0.25	1.39 ±0.43	1.57 ±0.43	1.55 ±0.22	1.40 ±0.42	1.21 ±0.47	1.47 ±0.46	1.96 ±0.39
S_v VES	0.14 ±0.03	0.14 ±0.04	0.09 ±0.03	0.09 ±0.01	0.07 ±0.02	0.06 ±0.03	0.05 ±0.01	0.07 ±0.01
V_v LY	0.81 ±0.43	0.57 ±0.32	0.47 ±0.35	0.20 ±0.09	0.04 ±0.06	0.21 ±0.20	0.04 ±0.08	0.17 ±0.22
V_v MCG	0.02 ±0.02	0.06 ±0.03	1.14 ±0.59	1.39 ±0.11	9.07 ±1.54	7.61 ±1.46	11.54 ±2.35	10.94 ±1.18
V_v FI	5.49 ±3.72	9.42 ±4.50	–	–	–	–	–	–
V_v FIB	140.00 ±12.00	176.00 ±35.00	244.00 ±31.00	264.00 ±40.00	265.00 ±29.00	287.00 ±14.00	235.00 ±12.00	250.00 ±34.00
V_v KH	–	–	–	–	–	–	52.80 ±4.39	45.66 ±11.83
V_v MEL	6.74 ±4.79	10.07 ±1.74	1.14 ±0.59	1.31 ±0.66	0.52 ±0.50	1.28 ±0.56	0.19 ±0.09	0.31 ±0.81
V_v GLY	0.02 ±0.04	–	0.68 ±0.92	0.76 ±0.80	0.11 ±0.09	0.22 ±0.33	–	–
V_v LD	1.54 ±2.22	0.41 ±0.35	0.04 ±0.04	0.15 ±0.12	0.09 ±0.08	–	–	0.03 ±0.04
V_v CGS	437.40 ±26.00	448.14 ±27.00	539.60 ±59.00	537.13 ±14.00	567.15 ±50.00	555.76 ±53.00	525.80 ±21.00	586.91 ±22.00
N/CY	0.42 ±0.06	0.41 ±0.13	0.20 ±0.12	0.15 ±0.06	0.14 ±0.07	0.12 ±0.07	0.04 ±0.02	0.08 ±0.03
SN/SPM	0.42 ±0.05	0.35 ±0.08	0.18 ±0.09	0.15 ±0.06	0.12 ±0.07	0.14 ±0.06	0.06 ±0.01	0.08 ±0.04
ND	12 ±3	15 ±3	40 ±4	36 ±4	51 ±15	41 ±2	47 ±12	46 ±4

[a] Surface densities (S_v) are expressed in m^2 per cm^3 of epidermal stratum, volume densities (V_v) in mm^3 per cm^3 of epidermal stratum, and the number of desmosomes (*ND*) is expressed per 100-μm^2 field. PM = plasma membrane; ICS = intercellular space; NK = nonkeratinocytes; N = nuclei; NM = nuclear membrane; CY = cytoplasm; MI = mitochondria; RIB = ribosomes; ER = endoplasmic reticulum; GO = Golgi apparatus; VES = vesicles; LY = lysosomes; MCG = membrane-coating granules; FI = filaments; FIB = filament bundles; KH = keratohyalin; MEL = melanosomes; GLY = glycogen; LD = lipid droplets; CGS = cytoplasmic ground substance; SN = surface of nucleus; SPM = surface of plasma membrane.

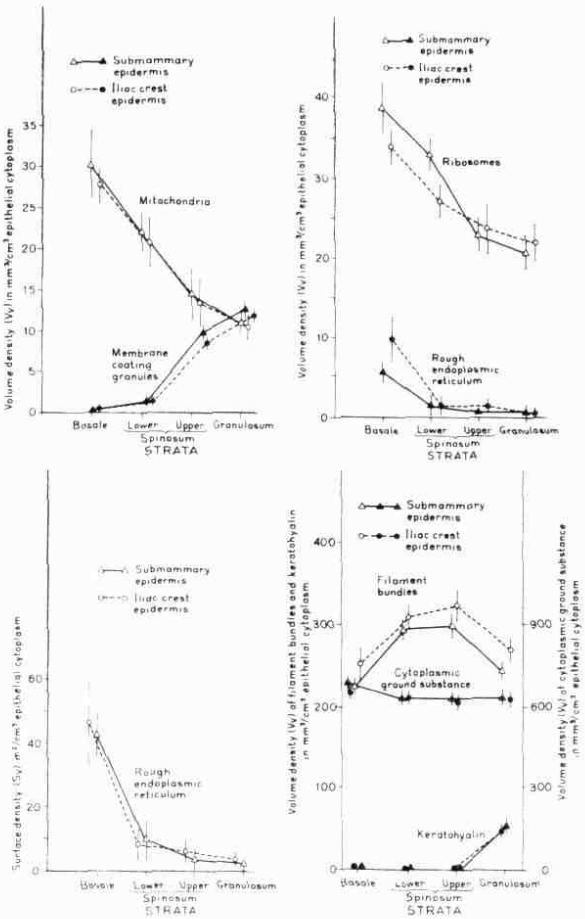

FIG. 2. Gradients of volume and surface density of several important cytoplasmic components.

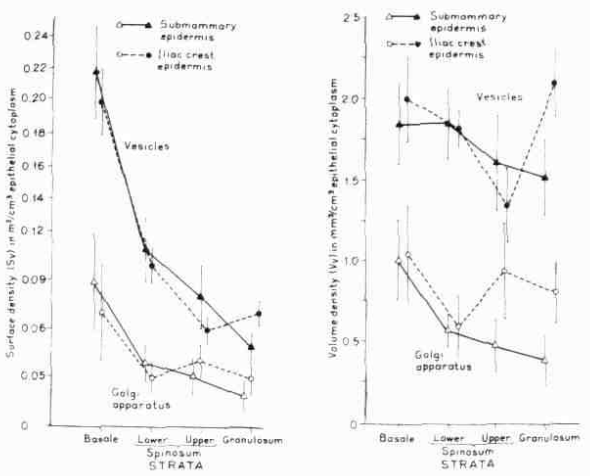

FIG. 3. Gradients of volume and surface density of Golgi apparatus and cytoplasmic vesicles.

son and better understanding of pathologically altered stratified squamous epithelia. Several authors have reported interesting numerical results employing nonstereologic morphometric techniques applied to some isolated parameters in sunlight-exposed and psoriatic epidermis [25,28,29]. These studies estimated, among other components, keratinosomes, desmosomes, and filaments. Comparison of these results between themselves and with the present data is difficult to carry out because different morphometric criteria, sampling techniques, and mathematical expressions were used.

Recently, modern stereologic methods have been applied to mouse [32,38] and rat epidermis,† normal human palate and buccal epithelia [37,38], and oral leukoplakias [40]. The data obtained by these authors fall in the same range of magnitudes as those here reported. Minor differences can be explained by variations in the ultrastructural criteria and in the species and epithelia studied.

The essential findings of the present stereologic analysis are in general agreement with previous qualitative studies [45–47], although in applying techniques of stereologic cytology, clear-cut numerical definitions of tissue and cell composition and of epithelial differentiation patterns are objectively obtained. In addition to this obvious advantage, it is hardly conceivable that the cytoplasmic ground substance which shows a plateau-like gradient throughout the strata in all keratinizing epithelia [37,41] and an exponential-like gradient in nonkeratinizing epithelia [38], could have been evaluated by methods other than stereology.

On the other hand, evaluation of certain components in sections that are thicker than the structures themselves, e.g., ribosomes, glycogen granules, and individual cytoplasmic filaments, is only approximate. This does not apply to filament bundles which are fairly gross ultrastructural constituents and usually thicker than ultrathin sections.

The stereologic study of epidermis in other regions of the human body with different structural and differentiation patterns as well as an analysis of the normal sex and age variations seems desirable before analyzing pathologic epithelia. In this way it would be possible to obtain valuable data on different diseases as has been the case while analyzing other tissues.

I wish to thank Dr. H. E. Schroeder, Department of Oral Structural Biology, University of Zurich, for his many helpful suggestions, and Mrs. A. M. Schneider and Miss K. Rossinsky for their expert technical assistance.

The generous cooperation of Drs. H. Obwegeser and W. Pepersack, Department of Maxillary Surgery, University of Zurich, who helped to provide the skin biopsies, is thankfully appreciated.

REFERENCES

1. Brody I: The ultrastructure of the epidermis in psoriasis vulgaris as revealed by electron microscopy. I. The dermo-epidermal junction and the stratum basale in parakeratosis without keratohyalin. J Ultrastruct Res 6:304–323, 1964
2. Nix TE Jr, Nordquist RE, Everett MA: Ultrastructural changes induced by ultraviolet light in human epidermis, granular and transitional layers. J Ultrastruct Res 12:547–573, 1965
3. Johnson FR, Fry L: Ultrastructural observations on lichen planus. Arch Dermatol 95:596–607, 1967
4. Brody I: The ultrastructure of the epidermis in lichen ruber planus as revealed by electron microscopy. II. Cytoplasm and nucleus in certain basal and spinous cells. J Ultrastruct Res 28:178–190, 1969

† de Rey BM, Cabrini RL, Klein-Szanto AJP: Stereology of irradiated epidermis (in preparation).

5. Nagy G, Janner M: Altersveränderugen in der menschlichen Epidermis. Eine elektronenmikroskopische Untersuchung. Arch Klin Exp Dermatol 238:70–86, 1970
6. Braun-Falco O: Die Dynamik der Hautreaktion nach Hornschichtabriss. Arch Dermatol Forsch 241:329–352, 1971
7. de Rey BM, Cabrini RL: Ultrastructural alteration in x-irradiated epidermis. J Invest Dermatol 60:137–149, 1973
8. Raick AN: Ultrastructural, histological and biochemical alterations produced by 12-O-tetradecanoylphorbol-13-acetate on mouse epidermis and their relevance to skin tumor promotion. Cancer Res 33:269–286, 1973
9. Tovell PWA, Weaver AC, Hope J, Sprott WE: The action of sodium lauryl sulphate on rat skin. An ultrastructural study. Br J Dermatol 90:501–506, 1974
10. Weibel ER, Bolender RP: Stereological techniques for electron microscopic morphometry, Principles and Technique of Electron Microscopy, vol 3. Edited by ME Hayat. New York, Van Nostrand-Rheinhold Co, 1973, pp 237–296
11. Weibel ER: Morphometry of the Human Lung. Heidelberg, Springer-Verlag, 1963
12. Loud AV: A quantitative stereological description of the ultrastructure of normal rat liver parenchymal cells. J Cell Biol 37:27–46, 1968
13. Weibel ER, Staubli W, Gnägi HR, Hess FA: Correlated morphometric and biochemical studies on the liver cell. I. Morphometric model stereologic methods, and normal morphometric data for rat liver. J Cell Biol 42:68–91, 1969
14. Rohr HP, Wirz A, Henning LC, Riede UN, Bianchi L: Morphometric analysis of rat liver cell in the perinatal period. Lab Invest 24:128–139, 1971
15. Bolender RP: Stereologic analysis of the guinea-pig pancreas. I. Analytical model and quantitative description of non-stimulated pancreatic exocrine cells. J Cell Biol 61:269–287, 1974
16. Page E, McCallister LP, Power B: Stereological measurements of cardiac ultrastructures implicated in excitation-contraction coupling. Proc Natl Acad Sci USA 68:1465–1466, 1971
17. Pinto JA, Brewer DB: Glomerular morphometry. I. Combined light and electron microscope studies in normal rats. Lab Invest 30:657–663, 1974
18. Wiener J, Loud AV, Kimberg DV, Spiro D: A quantitative description of cortisone-induced alterations in the ultrastructure of rat liver parenchymal cells. J Cell Biol 37:47–61, 1968
19. Stäubli W, Hess R, Weibel ER: Correlated morphometric and biochemical studies on the liver cell. II. Effects of phenobarbital on rat hepatocytes. J Cell Biol 42:92–112, 1969
20. McCallister LP, Page E: Effects of thyroxin on ultrastructure of rat myocardial cells. A stereologic study. J Ultrastruct Res 42:136–155, 1973
21. Rohr HP, Riede UN: Experimental metabolic disorders and the subcellular reaction pattern: morphometric analysis of hepatocytes. Curr Top Pathol 58:1–48, 1973
22. Weibel ER: A simplified morphometric method for estimating diffusing capacity in normal and emphysematous human lungs. Am Rev Resp Dis 107:579–588, 1973
23. Jorgensen M: A stereologic study of intrahepatic bile ducts. Congenital hepatic fibrosis. Acta Pathol Microbiol Scand [A] 82:21–29, 1974
24. Elfenbein IB, Baluarte HJ, Cubillos-Rojas TM, Gruskin AB, Coté M, Cornfeld D: Quantitative morphometry of glomerulonephritis with crescents. Diagnostic and predictive value. Lab Invest 32:56–64, 1975
25. Lagerkolm B: Cellular changes in the psoriatic epidermis. II. The submicroscopic organization in psoriatic lesions of different age. Acta Derm Venereol (Stockh) 45:99–122, 1965
26. Waterhouse JP, Squier CA: Measurements from electron micrographs of organelle size in relation to their shape: a refinement applied to the epidermal melanosome and basal lamella. J Microsc (Oxf) 89:195–204, 1968
27. Rupec M, Vakilzadeh F, Bruhl R: Die Haufigkeitsverteilung der Mitochondrien in der normalen Meerschweinchenepidermis. Eine quantitative elektronmikroskopische Untersuchung. Arch Klin Exp Dermatol 235:228–233, 1969
28. Wilgram GF, Kidd RL, Krawczyk WS, Coll PL: Sunburn effect on keratinosomes. A report with special note on ultraviolet-induced dyskeratosis. Arch Dermatol 101:505–511, 1970
29. Zelickson AS, Mottaz J: The effect of sunlight on human epidermis. A quantitative electron microscopic study of dendritic cells. Arch Dermatol 101:312–315, 1970
30. Sauter LS, Weibel ER: Morphometric evaluation of skin structures by stereologic methods. Application to testosterone-treated rats. Dermatologica 143:174–183, 1971
31. de Rey BM. Klein-Szanto AJP: A histometric study of acute radiation effects on rat tail epidermis. Strahlentherapie 143:699–704, 1972
32. Rowden G: Ultrastructural studies of keratinized epithelia of the mouse. III. Determination of the volumes of nuclei and cytoplasm of cells in murine epidermis. J Invest Dermatol 64:1–3, 1975
33. Rowden G: Ultrastructural studies of keratinized epithelia of the mouse. IV. Quantitative studies of lysosomes. J Invest Dermatol 64:4–8, 1975
34. Sauter LS, Loud AV: Morphometric evaluation of sebaceous gland volume in intact, castrated, and testosterone-treated rats. J Invest Dermatol 64:9–13, 1975
35. Schroeder HE, Munzel-Pedrazzoli S: Application of stereologic methods to stratified gingiva epithelia. J Microsc (Oxf) 92:179–198, 1970
36. Schroeder HE, Munzel-Pedrazzoli S: Morphometric analysis comparing junctional and oral epithelium of normal human gingiva. Helv Odontol Acta 14:53–66, 1970
37. Meyer M, Schroeder HE: A quantitative electron microscopic analysis of the keratinizing epithelium of normal human hard palate. Cell Tissue Res 158:177–203, 1975
38. Landay MA, Schroeder HE: Quantitative electron microscopic analysis of the non-keratinizing epithelium of normal human buccal mucosa. Cell Tissue Res (in press)
39. Klein-Szanto AJP, Schroeder HE: Architecture and density of the connective tissue papillae of the human oral mucosa. J Anat (in press)
40. Schroeder HE: Mucous membranes, Stereological Principles for Biomorphometry. Edited by ER Weibel. New York, Academic (in press)
41. Klein-Szanto AJP, Banoczy J, Schroeder HE: Metaplastic conversion of the differentiation pattern in oral epithelia affected by leukoplakia simplex. A stereologic study. Pathol Eur 11:189–210, 1976.
42. Karnovsky MJ: A formaldehyde-glutaraldehyde fixative of high osmolarity for use in electron microscopy. J Cell Biol 27:137a–138a, 1965
43. Luft JH: Improvements in epoxy resin embedding methods. J Biophys Biochem Cytol 9:409–414, 1961
44. Schroeder HE: Transmigration and infiltration of leukocytes in human junctional epithelium. Helv Odontol Acta 17:6–18, 1973
45. Odland GF, Reed TA: Epidermis, *in* Ultrastructure of Normal and Abnormal Skin. Edited by AS Zelickson. Philadelphia, Lea & Febiger, 1967, pp 54–75
46. Snell R: An electron microscopic study of the human epidermal keratinocyte. Z Zellforsch Mikrosk Anat 79:492–506, 1967
47. Breathnach A: An Atlas of Ultrastructure of Human Skin. Development, Differentiation and Post-Natal Features. London, J and A Churchill, 1971